Eur. Phys. J. B **10**, 385–396 (1999)

THE EUROPEAN PHYSICAL JOURNAL B

EDP Sciences

Towards lowering dissipation bounds for turbulent flows

R. Nicodemus[a], S. Grossmann, and Martin Holthaus[b]

Fachbereich Physik der Philipps-Universität, Renthof 6, 35032 Marburg, Germany

Received 26 October 1998

Abstract. We examine the background flow variational principle for calculating bounds on the energy dissipation rate in turbulent shear flow, and suggest to select this principle's test functions such that they comply with the small-scale smoothness of real turbulent velocity fields. A self-consistent algorithm implementing this requirement then yields an upper bound on the dimensionless dissipation coefficient which shows a weak power-law decrease at high Reynolds numbers, instead of approaching a nonzero constant, as it did in previous estimates.

PACS. 47.27.Nz Boundary layer and shear turbulence – 47.27.Jv High-Reynolds-number turbulence – 47.20.Ft Instability of shear flows

1 Introduction and motivation

Turbulent flow is an open nonequilibrium system, whose experimentally adjustable control parameter is the Reynolds number Re, and whose physical control parameter is the rate of energy that is fed into and dissipated by the flow. Hence the dependence of the energy dissipation rate ε on Re, which is the objective of this paper, is of prime importance.

To be specific, we consider a shear flow between two infinite parallel plates separated by a distance h; one of the plates being fixed and defining the plane $z = 0$ of a Cartesian coordinate system, the other one coinciding with the plane $z = h$ and being sheared with constant velocity U in the positive x-direction. The system thus exhibits translational invariance in the lateral, *i.e.*, y-direction. The Reynolds number is then defined as

$$Re = Uh/\nu, \tag{1}$$

where ν is the kinematic viscosity of the incompressible fluid. (Note that one frequently considers an arrangement where both plates are sheared against each other, one moving with velocity U, the other with $-U$, so that there is a neutral plane in the middle. In that case one denotes the distance between the plates as $2h$, but still defines the Reynolds number as $Re = Uh/\nu$ [1]. The entailing numerical value of Re is by a factor of four smaller than ours.)

The energy (per mass) dissipated by the flow, averaged over a time interval of length T and some suitable volume $\Omega = L_x L_y h$, is given by

$$\varepsilon_T \equiv \frac{1}{T}\int_0^T \mathrm{d}t \left\{ \frac{\nu}{\Omega}\int_\Omega \mathrm{d}^3x \left[\sum_{i,j=x,y,z} (\partial_j u_i)^2 \right] \right\} = \frac{\nu}{T}\int_0^T \mathrm{d}t \, \langle |\nabla \mathbf{u}|^2 \rangle, \tag{2}$$

where u_i $(i = x, y, z)$ denote the components of the fluid's Eulerian velocity field $\mathbf{u}(\mathbf{x}, t)$. As shown in equation (2), we employ angular brackets to indicate the spatial average. When measuring the long-time limit

$$\varepsilon \equiv \lim_{T\to\infty} \varepsilon_T \tag{3}$$

in multiples of $U^2/(hU^{-1})$, corresponding to the energy of the large eddies divided by the large-eddy turnover time, one obtains the dimensionless dissipation coefficient

$$c_\varepsilon(Re\,) \equiv \frac{\varepsilon}{U^3 h^{-1}}\,. \tag{4}$$

As long as Re remains less than about 1000, the flow between the plates remains laminar, *i.e.*, it exhibits a linear velocity profile,

$$\mathbf{u}(\mathbf{x}, t) = \mathbf{U}^{\mathrm{lam}}(\mathbf{x}) = U\frac{z}{h}\hat{\mathbf{x}}, \tag{5}$$

with $\hat{\mathbf{x}}$ denoting the unit vector in the x-direction. The corresponding dissipation coefficient can be calculated easily,

$$c_\varepsilon^{\mathrm{lam}}(Re\,) = Re^{-1}. \tag{6}$$

Beyond the onset of turbulence, $c_\varepsilon^{\mathrm{lam}}$ still has the quality of a rigorous lower bound [2], but the dissipation coefficient provided by the actual velocity field then becomes

[a] *Present address:* Robert Bosch GmbH, K1-Si/ECH5, Postfach 30 02 40, 70442 Stuttgart, Germany

[b] *Present address:* LMU München, Sektion Physik, Theresienstr. 37, 80333 München, Germany

significantly larger than Re^{-1}. The key question now is *whether $c_\varepsilon(Re)$ asymptotically approaches a nonzero constant, or whether it decreases to zero when Re becomes large*, and if so, how.

The data are inconclusive yet because of the limited range of Reynolds numbers accessible in laboratory experiments. Data from bulk measurements seem to be compatible with a dissipation coefficient that approaches a finite constant value [3], but other data for Taylor-Couette shear flow hint at a systematic decrease with increasing Re [4,5]. In the case of heat-driven Rayleigh–Bénard flow, c_ε (calculated from the measurements of the Nusselt number Nu [6,7]) obeys a power-law decrease up to Rayleigh numbers of the order of 10^{15}. Theory admits both: a $c_\varepsilon(Re)$ that approaches a finite value in the bulk, if one adheres to K41 turbulence [8], or $c_\varepsilon(Re) \propto Re^{-\kappa}$, where κ, taking on a value of about 0.035, measures the intermittency corrections in the second order structure function [9].

Clearly, information about the behavior of $c_\varepsilon(Re)$ carries interesting information about the structure of the turbulent flow. Therefore, mathematically rigorous *upper* bounds $\overline{c_\varepsilon}(Re)$ on $c_\varepsilon(Re)$ are of high relevance. Such bounds have been studied by Hopf [10], Howard [1], Busse (in the framework of his Optimum Theory [11,12]), Doering and Constantin (who have taken up the approach by Hopf and developed the "background flow method" [2,13,14]), and the present authors [15–19]. The main results obtained so far for turbulent shear flow can be summarized as follows: There is an asymptotic nonzero upper bound, $\overline{c_\varepsilon}(Re) \approx 0.01$ for $Re \to \infty$, first derived by Busse [11] and recently confirmed with higher precision as [17]

$$\overline{c_\varepsilon}(Re) = 0.010\,87(1) \qquad \text{for } Re \to \infty. \tag{7}$$

The latter work, based on an improved background flow variational principle [2,15], also provides a rigorous bound $\overline{c_\varepsilon}(Re)$ at finite Re. This bound exhibits some structure at the energy stability limit, related to the formation of the boundary layer and its separation from the bulk.

Although these two different approaches have led to the same asymptotic bound on c_ε, and could be shown to be equivalent [20], this is hardly the best, the ultimate answer. The present bound lies more than an order of magnitude above the various available data, and it shows no slight power-law decrease, as it could be implied by intermittent fluctuations [9], and as it seems to be present in some measured data [4,5,21]. Moreover, the structures observed at finite Re in the bound obtained in reference [17] appear to be an artifact brought about by a close relationship between the background flow method and energy stability theory. This latter theory [22–24] rests on a decomposition of the flow field into the laminar flow (5) and fluctuations around it,

$$\mathbf{u}(\mathbf{x},t) = \mathbf{U}^{\mathrm{lam}}(\mathbf{x}) + \mathbf{v}(\mathbf{x},t)\,, \tag{8}$$

leading to the evolution equation

$$\frac{1}{2}\frac{\mathrm{d}}{\mathrm{d}t}\langle \mathbf{v}^2\rangle = -\left(\frac{U}{h}\langle v_x v_z\rangle + \nu\,\langle|\nabla \mathbf{v}|^2\rangle\right) \tag{9}$$

for the fluctuations' energy. If the right hand side of this equation is strictly negative, the fluctuations fade away monotonously, irrespective of their initial value, so that the laminar flow is a globally attracting solution to the equations of motion. This is the case as long as the minimum of the bracketed expression in equation (9) remains positive, which, by means of the Rayleigh-Ritz variational principle, is guaranteed as long as all eigenvalues λ of the eigenvalue problem

$$\begin{aligned} \lambda \mathbf{V} &= -2\,h^2 \Delta \mathbf{V} + Re \begin{pmatrix} 0 & 0 & 1 \\ 0 & 0 & 0 \\ 1 & 0 & 0 \end{pmatrix} \mathbf{V} + \nabla P \\ 0 &= \nabla \cdot \mathbf{V} \end{aligned} \tag{10}$$

stay strictly positive; P is a Lagrange multiplier that takes the incompressibility condition into account. Positivity of all eigenvalues is ensured for Reynolds numbers below $Re_{\mathrm{ES}} \approx 82.65$, the energy stability limit, where the lowest eigenvalue passes through zero. However, this stability limit does *not* mark the onset of turbulence; the plane Couette flow becomes turbulent only at Reynolds numbers an order of magnitude higher than Re_{ES}. The key point is that this type of shear flow is linearly stable for all Re, so that the onset of turbulence is not related to the loss of linear stability, but rather due to a nonlinear-nonnormal transition mechanism [25–28]; a comprehensive discussion of this true transition mechanism can be found in reference [29]. Since the presently existing variational principle [15] does incorporate energy stability theory (as will become obvious later), but not the dynamical features which actually govern the onset of turbulence, the bound on the energy dissipation rate derived from this principle is significantly too high at finite Re: It separates from the laminar behavior (6) already at the energy stability limit, although realistic flows suffer the emergence of permanent turbulence only for much higher Re.

There is an immediate theoretical reason why also the long-standing *asymptotic* bound on c_ε (Busse's value was established in 1970) might not be as sharp as intended. Both the Optimum Theory and the Background Flow approach, though based on the Navier–Stokes equation of motion, bound functionals of the velocity field in the space of *all* incompressible vector fields that comply with the proper boundary conditions, rather than restricting these functionals to the actual solutions of the equations of motion. Hence, characteristic properties and the structure of real turbulent flows are not adequately taken into account.

The aim of the present paper is to point out that the variational upper bound on $c_\varepsilon(Re)$ can indeed be lowered if essential properties of actual Navier–Stokes solutions, and hence of realistic turbulent flows, are respected in the choice of the admitted test functions. As explained in detail in the following section, a test function is admitted to the background flow variational principle if a certain functional provided by that test function stays positive definite in the entire space of divergence-free vector fields with homogeneous boundary conditions. We weaken this restriction by requiring that the functional in question be positive definite *only on the manifold of vector fields whose*

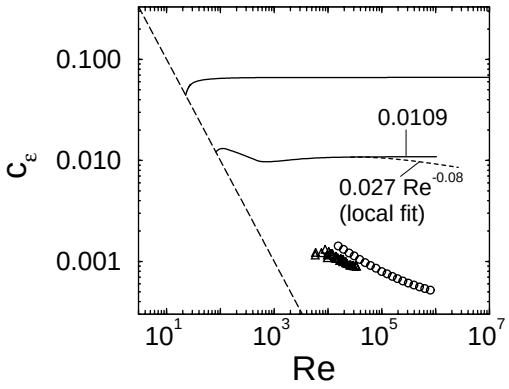

Fig. 1. Bounds on the dissipation coefficient $c_\varepsilon(Re)$ in comparison with experimental data. Slanted dashed line: lower bound (6) provided by the laminar flow. Uppermost solid line: upper bound obtained in reference [15] from an analytical evaluation of the variational principle, employing an over-restrictive constraint for the test profiles. This bound approaches $3/(32\sqrt{2}) \approx 0.0663$ for $Re \to \infty$. Lower solid line: upper bound obtained in reference [17]; this bound approaches the asymptotic value (7). Dashed line bifurcating from that bound: upper bound computed in this work. The numerical data are well fitted by $\overline{c_\varepsilon}(Re) \approx 0.027 \times Re^{-0.08}$; however, the asymptotic value of the exponent is $-0.18(1)$. Circles: data measured by Lathrop *et al.* for a small-gap Taylor-Couette flow [4,5]. Triangles: data measured by Reichardt for a plane Couette flow [21].

fluctuation length scale exceeds the inner length scale of turbulence, which is of the order of the Kolmogorov length η. Hence, more test functions are admitted to the variational principle (more precisely, a given test function becomes admissible up to higher Reynolds numbers), which, in turn, leads to a systematic lowering of the dissipation bound. We find a weak power-law decrease of the resulting new bound,

$$\overline{c_\varepsilon}(Re) \propto Re^{-\alpha}, \tag{11}$$

with $\alpha \approx 0.08$ for Reynolds numbers of the order of 10^6. The analysis of our numerical data, summarized in Appendices A and B, shows that this exponent has merely a local validity; in the regime of asymptotically high Re it even increases up to about 0.18. However, this asymptotic regime is reached only at Reynolds numbers beyond 10^{20}, so that the local exponent might have more physical significance than the asymptotic one. As shown in Figure 1, the numerical improvement on the previous bound is only minute for $Re \approx 10^6$, and the new bound still does not correctly describe the experimental findings, but the fact that this bound tends to zero asymptotically, and thus goes below all previously computed bounds, is of principal importance.

We hasten to add that the weakening of the constraint imposed on the admitted test functions is physically plausible, but it is not based on rigorous mathematical inequalities. In this sense, the improved bound on $c_\varepsilon(Re)$ computed in this paper does not rest on the same mathematically impeccable foundation as its precursors derived in references [11,17]. However, our *ad-hoc* modification of the variational principle is backed by indisputable physical facts, and the distinct value of our non-rigorous argument is that it shows in a paradigmatic manner just how respecting generic properties of turbulent flows can translate into improved, physically meaningful dissipation bounds.

In the following section we scrutinize the background flow variational principle [2,15] in detail, in order to elucidate both its strength and its weakness on a technical level. This provides the necessary background for Section 3, where we suggest a scheme for incorporating the small-scale smoothness of real turbulent velocity fields into the variational principle, and present numerical data that establish the bound (11). In the final Section 4 we discuss some general features of our solution.

2 Criticism of the variational principle

The technical discussion of the variational principle for calculating upper bounds on the energy dissipation rate, and of its modification, starts with the Hopf decomposition of the turbulent velocity field $\mathbf{u}(\mathbf{x},t)$ into an auxiliary, stationary field $\mathbf{U}(\mathbf{x})$, dubbed the "background flow field" by Doering and Constantin [2], and the deviations $\mathbf{v}(\mathbf{x},t)$ from that field,

$$\mathbf{u}(\mathbf{x},t) = \mathbf{U}(\mathbf{x}) + \mathbf{v}(\mathbf{x},t)\,. \tag{12}$$

At this point, the auxiliary field is not specified any further (in particular, it should neither be misinterpreted as some sort of average of the actual flow, nor does it have to coincide with a stationary solution to the equations of motion, as it did in the decomposition (8) underlying energy stability theory), except that we require [2,10] that it has to carry the no-slip boundary conditions of $\mathbf{u}(\mathbf{x},t)$, *i.e.*, $\mathbf{U}(x,y,0,t) = \mathbf{0}$ and $\mathbf{U}(x,y,h,t) = U\hat{\mathbf{x}}$ for all x, y, and t. In addition, we impose periodic boundary conditions in both the x- and y-direction. Hence, the deviations $\mathbf{v}(\mathbf{x},t)$ satisfy homogeneous boundary conditions, so that $\mathbf{v}(x,y,0,t) = \mathbf{0}$ and $\mathbf{v}(x,y,h,t) = \mathbf{0}$, together with periodic boundary conditions in x and y. (Throughout this paper, we will use lowercase boldface letters for time-dependent vector fields like $\mathbf{u}$, whereas uppercase symbols refer to stationary fields, such as $\mathbf{U}$.) The dynamics of the incompressible flow are governed by the Navier–Stokes equations

$$\begin{aligned} \partial_t \mathbf{u} + \mathbf{u}\cdot\nabla\mathbf{u} + \nabla p &= \nu\,\Delta\mathbf{u} \\ \nabla\cdot\mathbf{u} &= 0, \end{aligned} \tag{13}$$

where p is the kinetic pressure.

Plugging the decomposition (12) into these equations, dotting with $\mathbf{v}$, and spatially averaging over the periodicity volume Ω immediately leads to

$$\begin{aligned} \frac{1}{2}\frac{\mathrm{d}}{\mathrm{d}t}\langle\mathbf{v}^2\rangle + \langle\mathbf{v}\cdot(\mathbf{U}\cdot\nabla\mathbf{U})\rangle + \langle\mathbf{v}\cdot(\nabla\mathbf{U})_{\mathrm{sym}}\cdot\mathbf{v}\rangle \\ = -\nu\,\langle\nabla\mathbf{U}\cdot\nabla\mathbf{v}\rangle - \nu\,\langle|\nabla\mathbf{v}|^2\rangle, \end{aligned} \tag{14}$$

with the components of the symmetric tensor $(\nabla\mathbf{U})_{\rm sym}$ being given by $[(\nabla\mathbf{U})_{\rm sym}]_{i,j} \equiv \frac{1}{2}(\partial_i U_j + \partial_j U_i)$. This is the only step in the entire reasoning where the Navier–Stokes equations are utilized directly. On the other hand, we have the obvious identity

$$\nu\,\langle|\nabla\mathbf{u}|^2\rangle = \nu\,\langle|\nabla\mathbf{U}|^2\rangle + 2\nu\,\langle\nabla\mathbf{U}\cdot\nabla\mathbf{v}\rangle + \nu\,\langle|\nabla\mathbf{v}|^2\rangle. \quad (15)$$

Multiplying equation (14) by a dimensionless balance parameter $a > 1$, adding equation (15), averaging over some time interval of length T, and then taking the limit $T \to \infty$ results in the exact inequality [15]

$$\varepsilon \le \nu\,\langle|\nabla\mathbf{U}|^2\rangle - a\,\liminf_{T\to\infty}\left\{\frac{1}{T}\int_0^T {\rm d}t\Big\langle\frac{a-1}{a}\nu\,|\nabla\mathbf{v}|^2 + \mathbf{v}\cdot(\nabla\mathbf{U})_{\rm sym}\cdot\mathbf{v} + \mathbf{F}\cdot\mathbf{v}\Big\rangle\right\}, \quad (16)$$

where

$$\mathbf{F} \equiv \mathbf{U}\cdot\nabla\mathbf{U} - \frac{a-2}{a}\nu\,\Delta\mathbf{U}. \quad (17)$$

This inequality (16) is not strong, in the sense that it reduces to an identity if the $T \to \infty$-limit of the time-average exists (*i.e.*, if the lim inf is equal to the lim sup), which appears to be not unlikely.

At this point, we have bounded the dissipation rate by the simple expression $\nu\,\langle|\nabla\mathbf{U}|^2\rangle$ which depends solely on the still arbitrary auxiliary field $\mathbf{U}$, plus a functional of the deviations $\mathbf{v}$, and the task now is to control that functional. Certainly, the integral on the right hand side of the inequality (16) is larger than or equal to the expression which is obtained if the actual deviations $\mathbf{v}(\mathbf{x},t)$, which still reflect the full Navier–Stokes dynamics, are replaced by that stationary velocity field which minimizes the integrand:

$$\frac{1}{T}\int_0^T {\rm d}t\,\left\langle\frac{a-1}{a}\nu\,|\nabla\mathbf{v}|^2 + \mathbf{v}\cdot(\nabla\mathbf{U})_{\rm sym}\cdot\mathbf{v} + \mathbf{F}\cdot\mathbf{v}\right\rangle \ge \inf_{\mathbf{V}}\left\{\left\langle\frac{a-1}{a}\nu\,|\nabla\mathbf{V}|^2 + \mathbf{V}\cdot(\nabla\mathbf{U})_{\rm sym}\cdot\mathbf{V} + \mathbf{F}\cdot\mathbf{V}\right\rangle\right\}. \quad (18)$$

This is the decisive step. Even if the actual deviation $\mathbf{v}(\mathbf{x},t)$ comes momentarily close to the minimizing field during the course of time, it is highly unlikely that it does so at almost all times. But only under this condition could the estimate (18) be sharp. In short, by adopting this estimate we sacrifice the Navier–Stokes dynamics and thus gain mathematical simplicity and rigor, but we lose sharpness: It is clear that this estimate will allow us to compute a bound on the dissipation rate in a relatively straightforward manner, *i.e.*, without having to solve the equations of motion, but we cannot *a priori* know how close that bound will come to the dissipation rate of real turbulent shear flow.

However, the situation might not be too bad, since the minimizing field in the estimate (18) still depends on the yet unspecified auxiliary field $\mathbf{U}$, so that the bound on ε furnished by the two inequalities (16) and (18) can be optimized, *i.e.*, made as low as the scheme permits, by varying $\mathbf{U}$. This constitutes the strength of the approach: *Any* $\mathbf{U}$ yields a bound on ε, as long as Re remains sufficiently low; the hope is that by choosing optimal $\mathbf{U}$-fields one might be able to construct a bound that captures significant features of the experimentally measured dissipation rate.

For carrying through this program, we first have to find, for each given $\mathbf{U}$, the minimizing field in the estimate (18), denoted as $\mathbf{W} = \mathbf{W}\{\mathbf{U}\}$. Assuming that $\mathbf{F}$ is no gradient [15], this field has to satisfy the Euler–Lagrange equations

$$\begin{aligned}\mathbf{0} &= -2\frac{a-1}{a}\nu\,\Delta\mathbf{W} + 2\,(\nabla\mathbf{U})_{\rm sym}\cdot\mathbf{W} + \nabla P + \mathbf{F}\\ 0 &= \nabla\cdot\mathbf{W}\,,\end{aligned} \quad (19)$$

where the Lagrange multiplier P accounts for divergence-freeness; homogeneous boundary conditions are understood. In order to guarantee that the solution $\mathbf{W}$ to this equation is unique, and indeed leads to a *minimum* in the estimate (18), the functional

$$H_{a,\mathbf{U}}\{\mathbf{V}\} \equiv \left\langle\frac{a-1}{a}\nu\,|\nabla\mathbf{V}|^2 + \mathbf{V}\cdot(\nabla\mathbf{U})_{\rm sym}\cdot\mathbf{V}\right\rangle \quad (20)$$

has to be strictly positive definite. This is equivalent to the requirement that all eigenvalues λ of the linear eigenvalue problem

$$\begin{aligned}\lambda\mathbf{V} &= -2\frac{a-1}{a}\nu\,\Delta\mathbf{V} + 2\,(\nabla\mathbf{U})_{\rm sym}\cdot\mathbf{V} + \nabla P\\ 0 &= \nabla\cdot\mathbf{V}\end{aligned} \quad (21)$$

be strictly positive. If this crucial condition is not satisfied, the chosen $\mathbf{U}$ cannot yield a bound, since the second term in the inequality (16) cannot be controlled. In that case the particular $\mathbf{U}$ has to be discarded and to be replaced by a more promising one. But if all eigenvalues of (21) are strictly positive, then computing a bound is an easy matter: The estimate (18) becomes

$$\frac{1}{T}\int_0^T {\rm d}t\Big\langle\frac{a-1}{a}\nu\,|\nabla\mathbf{v}|^2 + \mathbf{v}\cdot(\nabla\mathbf{U})_{\rm sym}\cdot\mathbf{v} + \mathbf{F}\cdot\mathbf{v}\Big\rangle \ge \frac{1}{2}\langle\mathbf{F}\cdot\mathbf{W}\rangle, \quad (22)$$

and the bounding inequality (16) finally yields the variational inequality [15]

$$\varepsilon \le \inf_{a>1,\,\mathbf{U}}\Big\{\nu\,\langle|\nabla\mathbf{U}|^2\rangle - \frac{a}{2}\,\langle\mathbf{W}\cdot(\mathbf{U}\cdot\nabla\mathbf{U})\rangle + \frac{1}{2}(a-2)\nu\,\langle\mathbf{W}\cdot\Delta\mathbf{U}\rangle\Big\}. \quad (23)$$

When applying this general scheme to the plane shear flow described in the Introduction, the geometry of the problem suggests the restriction to auxiliary fields $\mathbf{U}$ that are determined by a one-dimensional profile function $\phi(\zeta)$,

$$\mathbf{U}(\mathbf{x}) = U\phi(\zeta)\,\hat{\mathbf{x}}\,, \tag{24}$$

where $\zeta = z/h$ is the dimensionless height coordinate. The no-slip boundary conditions imposed on the auxiliary field translate into $\phi(0) = 0$ and $\phi(1) = 1$. The profile functions ϕ thus become test functions for the variational principle (23). The eigenvalue problem (21), which decides by the sign of its eigenvalues whether or not a given test function is admissible for computing a bound on the dissipation rate, adopts the form

$$\begin{aligned} \lambda\mathbf{V} &= -2\,h^2\Delta\mathbf{V} + R\,\phi'\begin{pmatrix} 0&0&1\\ 0&0&0\\ 1&0&0 \end{pmatrix}\mathbf{V} + \nabla P \\ 0 &= \nabla\cdot\mathbf{V}, \end{aligned} \tag{25}$$

where

$$R \equiv \frac{a}{a-1}\,Re. \tag{26}$$

If one tries the laminar profile $\phi(\zeta) = \zeta$, yielding the constant slope $\phi'(\zeta) = 1$, this eigenvalue problem becomes exactly equal to the problem (10) already encountered in the energy stability theory of the plane Couette flow, except for the replacement of the Reynolds number Re by the rescaled Reynolds number (26). Hence, for $\phi(\zeta) = \zeta$ all eigenvalues of (25) will remain positive — the laminar profile will remain an admissible test function for the variational principle — as long as R remains below the energy stability limit $Re_{\mathrm{ES}} \approx 82.65$. The maximal Reynolds number Re compatible with this value of R, namely Re_{ES}, is then found by setting $a = \infty$, so that the laminar profile remains admissible for Reynolds numbers up to $Re = Re_{\mathrm{ES}}$. In this way it is shown that for $Re \le Re_{\mathrm{ES}}$ the laminar dissipation coefficient (6) provides not only a lower, but also an upper bound on c_ε.

The case of the laminar test profile illustrates that the eigenvalue problem (25) constitutes a generalization of energy stability theory: Just as the laminar profile defines the energy stability limit, also every other, arbitrarily chosen test profile $\phi(\zeta)$ defines a "critical" value $R_{\mathrm{c}}\{\phi\}$ where the lowest eigenvalue of the corresponding problem (25) becomes negative. (Since $-\Delta$ is positive definite, each ϕ will yield only positive eigenvalues for sufficiently small R.) Setting $a = \infty$, this value $R_{\mathrm{c}}\{\phi\}$ corresponds to the maximal Reynolds number Re up to which this ϕ remains admissible; for $Re > R_{\mathrm{c}}\{\phi\}$ it has to be discarded.

When considering only auxiliary fields $\mathbf{U}$ of the form (24), the Euler–Lagrange equations (19) for the minimizing field $\mathbf{W}$ can be solved analytically in terms of the respective profile ϕ [15]. After $R_{\mathrm{c}}\{\phi\}$ has been determined, the optimization of the balance parameter a can be performed. Introducing the profile functional

$$D\{\phi\} \equiv \int_0^1 \mathrm{d}\zeta\,[\phi'(\zeta)]^2 - 1, \tag{27}$$

which quantifies how strongly ϕ differs from the laminar profile, the bound produced by a particular profile ϕ can be written as

$$c_\varepsilon(Re\,) \le \begin{cases} [1 + D\{\phi\}]\,Re^{-1} \\ \qquad \text{for} \quad 0 \le Re < \dfrac{1}{2}R_{\mathrm{c}}\{\phi\} \\ \left[1 + \dfrac{D\{\phi\}\,R_{\mathrm{c}}\{\phi\}^2}{4\,(R_{\mathrm{c}}\{\phi\} - Re)\,Re}\right] Re^{-1} \\ \qquad \text{for} \quad \dfrac{1}{2}R_{\mathrm{c}}\{\phi\} \le Re < R_{\mathrm{c}}\{\phi\}\,; \end{cases} \tag{28}$$

the optimal bound $\overline{c_\varepsilon}(Re\,)$ obtainable from the profile's variation corresponds to the lower envelope of the individual graphs (28). It should be noted that each such graph is continuous, and even continuously differentiable, at $Re = \frac{1}{2}R_{\mathrm{c}}\{\phi\}$.

The asymptotic bound (7) has been derived in precisely this manner. That bound is mathematically rigorous, but the fact that it lies still an order of magnitude above the experimental data is disappointing, to say the least. In particular, it remains unclear whether also the true dissipation coefficient c_ε becomes asymptotically constant, or whether the method is simply not powerful enough to capture a possibly existing asymptotic decrease to zero. Obviously, the price paid for abandoning the Navier–Stokes dynamics in the estimate (18) was too high; the hope that one could at least partially compensate for this sacrifice by exploiting the freedom to adjust the auxiliary field was overly optimistic. It appears that the bound on the dissipation rate can only be improved if one succeeds in preserving some characteristic properties of real turbulent flows, all of which still enter on the left hand side of the estimate (18), when going to the right hand side of that inequality. Seeking the infimum over *all* stationary, divergence-free vector fields $\mathbf{V}(\mathbf{x})$ with homogeneous boundary conditions is — albeit mathematically convenient — too strong an estimate with respect to the actual physics; it should be sufficient to seek the infimum only within a restricted class of fields that share essential properties of the physically realized turbulent deviations $\mathbf{v}(\mathbf{x}, \mathbf{t})$. The infimum within that restricted class should (hopefully) be *higher* than that pertaining to the full set of all $\mathbf{V}$, hence one subtracts *more* from the first term in the bounding inequality (16) — the bound is lowered.

3 Modification of the variational principle

The property of real turbulent flows which we focus on in the present first attempt to make the above deliberations work is their smoothness on length scales below the "inner" scale of turbulence, which is of the order of the Kolmogorov length

$$\eta = (\nu^3/\varepsilon)^{1/4}. \tag{29}$$

More precisely, one meets the transition from the viscosity-dominated, "viscous" subrange where the flow is

smooth to the inertial subrange where it is determined by convection at $\ell \approx 10\,\eta$ [30]; a turbulent velocity field contains eddies with all sizes between the "outer" scale h and $10\,\eta$, but, except for occasional fluctuations, no smaller ones.

To see how to incorporate this basic fact into the variational principle, we need to recapitulate some of the technical details encountered when checking the admissibility of a test profile ϕ [17,18]. Exploiting the periodic boundary conditions in the x-y-plane, the eigenvectors $\mathbf{V}$ and the Lagrange multiplier P entering into the eigenvalue problem (25) are written as

$$\begin{aligned} \mathbf{V}(\mathbf{x}) &= \widetilde{\mathbf{V}}(z)\,\mathrm{e}^{\mathrm{i}(k_x x + k_y y)} \\ P(\mathbf{x}) &= \widetilde{P}(z)\,\mathrm{e}^{\mathrm{i}(k_x x + k_y y)}. \end{aligned} \tag{30}$$

Hence, the eigenvalue problem adopts the form

$$\begin{aligned} \lambda\,\widetilde{V}_x &= -2\,h^2\left(\partial_z^2 - k^2\right)\widetilde{V}_x + R\,\phi'\,\widetilde{V}_z + \mathrm{i}\,k_x\widetilde{P} \\ \lambda\,\widetilde{V}_y &= -2\,h^2\left(\partial_z^2 - k^2\right)\widetilde{V}_y + \mathrm{i}\,k_y\widetilde{P} \\ \lambda\,\widetilde{V}_z &= -2\,h^2\left(\partial_z^2 - k^2\right)\widetilde{V}_z + R\,\phi'\,\widetilde{V}_x + \partial_z\widetilde{P} \\ 0 &= \mathrm{i}\,k_x\widetilde{V}_x + \mathrm{i}\,k_y\widetilde{V}_y + \partial_z\widetilde{V}_z, \end{aligned} \tag{31}$$

with $k \equiv \sqrt{k_x^2 + k_y^2}$; the boundary conditions read $\widetilde{\mathbf{V}}(0) = \widetilde{\mathbf{V}}(h) = \mathbf{0}$. For a given profile ϕ and fixed wave numbers k_x and k_y, one first determines that value $R_0\{\phi\}(k_x, k_y)$ for which the lowest eigenvalue λ becomes zero; the desired value $R_\mathrm{c}\{\phi\}$, which according to the previous section corresponds to the maximal Reynolds number Re up to which ϕ remains an admissible test profile, is then found by minimizing over all wave numbers:

$$R_\mathrm{c}\{\phi\} = \min_{k_x \geq 0,\, k_y > 0} \{R_0\{\phi\}(k_x, k_y)\}\cdot \tag{32}$$

As a convenient class of test profiles, which is likely to exhaust the variational principle at least for high Reynolds numbers [19], we propose

$$\phi(\zeta) = \begin{cases} \dfrac{1}{2}\,(1-p) + p\,\zeta - \dfrac{1}{2}\,(1-p)\,(1-\zeta/\delta)^n \\ \qquad\qquad \text{for} \quad 0 \leq \zeta \leq \delta \\ \dfrac{1}{2}\,(1-p) + p\,\zeta \\ \qquad\qquad \text{for} \quad \delta < \zeta < 1-\delta \\ \dfrac{1}{2}\,(1-p) + p\,\zeta + \dfrac{1}{2}\,(1-p)\,(1-(1-\zeta)/\delta)^n \\ \qquad\qquad \text{for} \quad 1-\delta \leq \zeta \leq 1. \end{cases} \tag{33}$$

These profiles are parameterized by the slope p in the interior, with $0 < p \leq 1$, the polynomial order $n \geq 4$, and the dimensionless width δ of the boundary segments, $0 < \delta \leq 1/2$; they are $n-1$ times continuously differentiable at the matching points. Determining $R_\mathrm{c}\{\phi\}$ for each member of this set of profiles, computing the graphs (28), and constructing their lower envelope, *i.e.*, the optimal upper bound $\overline{c_\varepsilon}(Re\,)$ for the dissipation coefficient, one finds that for each Reynolds number Re the minimizing wave number k_x that belongs to the optimal profile is equal to zero [17]. The minimizing wave numbers k_y corresponding to the respective optimized profiles show a more subtle behavior: There is a single, nonzero minimizing k_y for $Re \leq Re_\mathrm{B} \approx 460$, which bifurcates at Re_B and thus gives rise to two separate branches of minimizing wave numbers at higher Re. One of these branches, referred to as $k_{y,1}$, becomes asymptotically constant, the other one, denoted as $k_{y,2}$ in the following, scales proportionally to Re.

From the technical viewpoint, the occurrence of two minimizing wave numbers reflects a degeneracy of the eigenvalue problem (25): Above Re_B, two eigenvalues pass through zero simultaneously. This manifests itself in the fact that $R_0\{\phi\}(0, k_y)$, considered as function of k_y for a profile ϕ that is optimal at some particular Re_0, possesses a double minimum; the common value

$$R_0\{\phi\}(0, k_{y,1}) = R_0\{\phi\}(0, k_{y,2}) \tag{34}$$

obviously equals $R(Re_0)$, *i.e.*, that rescaled Reynolds number (26) which belongs to the Reynolds number Re_0 at which the profile is optimal. (If it were lower, ϕ would not be admissible at Re_0; if it were higher, another ϕ would produce a lower bound at Re_0.) The equality (34) thus expresses one of the most characteristic features of the variational principle. (If the eigenvalue problem (25) should possess an even higher degeneracy, as one might perhaps guess on the grounds of Busse's multi-α-solutions to the variational problem occurring in the Optimum Theory [11,12], then a suitable class of test profiles, more sophisticated than (33), would lead to multiple minima of the corresponding functions $R_0\{\phi\}(0, k_y)$. Nonetheless, the value of each minimum would have to be precisely $R(Re_0)$, as in our case).

From the physical viewpoint, the two minimizing branches of wave numbers reflect two characteristic length scales of the optimized profiles: $2\pi/k_{y,1} \propto Re^0$ corresponds to the length of the interior segment where the optimized profiles become flat; $2\pi/k_{y,2} \propto Re^{-1}$ corresponds to the extension of the segments close to the boundaries at $\zeta = 0$ and $\zeta = 1$ where the profiles become steep [17,19]. It is this second, shrinking length scale which is physically objectionable. Namely, the Kolmogorov length (29) can be written in the form

$$\eta/h = \left(c_\varepsilon Re^3\right)^{-1/4}\ ; \tag{35}$$

η thus decreases as $Re^{-3/4}$ if the true dissipation coefficient c_ε approaches a nonzero constant, and even weaker if c_ε decreases slightly with Re. Since, on the other hand, $2\pi/k_{y,2}$ decreases as Re^{-1}, the extension of the profiles' steep boundary segments will, at sufficiently high Reynolds numbers, inevitably become smaller than $10\,\eta$. When that happens, the bound $\overline{c_\varepsilon}$ provided by the variational principle is determined by an eigenvector $\mathbf{V}$ which is characterized by a wave number k_y larger than $2\pi/(10\,\eta)$, *i.e.*, by an eigenvector belonging to a subset of $\mathbf{V}$-space which is, supposedly, not visited by the turbulent deviations $\mathbf{v}(\mathbf{x}, t)$ — always assuming, of course,

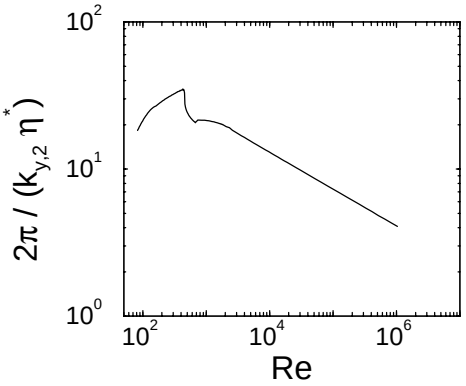

Fig. 2. Length scale $2\pi/k_{y,2}$, corresponding to the upper branch of minimizing wave numbers for the variational bound displayed in Figure 1, in multiples of the auxiliary length η^*, see equation (36). The ratio $2\pi/(k_{y,2}\,\eta^*)$ decreases as $Re^{-1/4}$ at large Reynolds numbers. At about $Re = 3 \times 10^4$, it drops below 10.

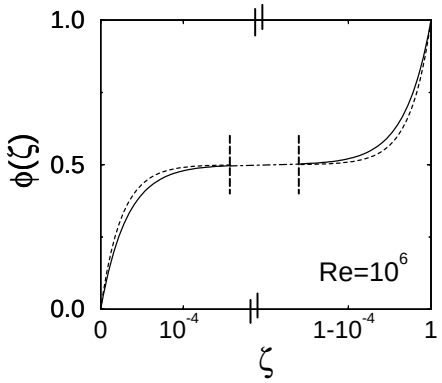

Fig. 3. Optimized test profiles, for $Re = 10^6$, as resulting from the original variational principle that does not take the Kolmogorov length into account (dashed), and from the self-consistently modified principle (full line; $b = 10$). The latter principle yields profiles which are slightly less steep in the vicinity of the boundaries. Note the break of the scale of the abscissa.

that the auxiliary field $\mathbf{U}$ is sufficiently smooth. Then the spectral constraint imposed on the test profiles is overly restrictive and should be weakened.

Since the true dissipation coefficient c_ε, and hence the true Kolmogorov length η, is not at our disposal, we define an auxiliary length η^* according to

$$\eta^*/h \equiv \left(\overline{c_\varepsilon} Re^3\right)^{-1/4}, \tag{36}$$

with $\overline{c_\varepsilon}$ as provided by the variational principle. Since $c_\varepsilon \le \overline{c_\varepsilon}$, we have $\eta^* \le \eta$. Hence, when $2\pi/k_{y,2}$ drops below $10\,\eta^*$, then it is *a fortiori* smaller than $10\,\eta$, the length scale marking the transition from the inertial to the viscous subrange.

Figure 2 shows the ratio $2\pi/(k_{y,2}\,\eta^*)$ corresponding to the asymptotically constant bound $\overline{c_\varepsilon}$ obtained in reference [17], which had already been displayed in Figure 1. At about $Re = 3 \times 10^4$ this ratio passes the value 10, so that the bound becomes determined by an eigenvector with unphysically small spatial structure. To remedy this deficiency, we employ the following algorithm:

(i) For each Reynolds number Re, the upper bound $\overline{c_\varepsilon}(Re\,)$ provides a length scale η^* according to equation (36).

(ii) Given η^*, we define the maximal wave number admitted,

$$\frac{k^*_{y,2}}{2\pi} \equiv \frac{1}{b\,\eta^*}, \tag{37}$$

with a cutoff parameter b set equal to 10, following the insight that the transition to the viscous subrange occurs at about $10\,\eta$. (Note that this is a worst-case estimate, since we are not working with the true Kolmogorov length η, but rather with the smaller η^*.) In order to check the dependence of our results on the cut-off parameter, we will also consider the values $b = 5$ and $b = 20$.

(iii) We then adjust the variational profiles such that the characteristic identity (34) is satisfied with $k^*_{y,2}$ instead of the previous $k_{y,2}$,

$$R_0\{\phi\}\big(0, k^*_{y,1}\big) = R_0\{\phi\}\big(0, k^*_{y,2}\big)\,; \tag{38}$$

the new lower minimizing wave number $k^*_{y,1}$ again has to be determined by a minimum search. In this way, we restrict the wave numbers k_y of the eigenvectors which belong to the lowest eigenvalue of (25) at its passage through zero to values less than $2\pi/(b\,\eta^*)$, thus mimicking the small-scale smoothness of the turbulent deviations $\mathbf{v}(\mathbf{x}, t)$.

(iv) Going through the already familiar lower-envelope procedure [17,18], we construct a new bound $\overline{c_\varepsilon}(Re\,)$ and then step back to i): The new bound yields a new value η^*, which, in its turn, gives a new wave number $k^*_{y,2}$, and so forth. Iterating this scheme, η^*, $k^*_{y,2}$, and $\overline{c_\varepsilon}$ are found to converge fairly rapidly, until in the end the equations (36), (37), and (38) are satisfied simultaneously.

Though this self-consistent procedure is rather intricate as far as the numerical effort is concerned, its essence is fairly simple: Since the admissibility of the profiles ϕ is no longer tested for all wave numbers, but only for that subset which complies with the smoothness of turbulent flows at scales below $10\,\eta^*$, the limits of admissibility $R_c\{\phi\}$ are increased, so that the lower envelope of the graphs (28) decreases. A comparison of optimized profiles as provided by the original variational principle and its self-consistent descendant is depicted in Figure 3; as expected, the latter are less steep in the vicinity of the boundaries.

It may be helpful to spell out the hypothesis underlying the construction of the new bound in mathematical terms. A self-consistently computed profile ϕ, which leads to a lowering of the previous bound, would not have passed the original admissibility criterion; it gives rise to (possibly many) negative eigenvalues of the problem (25) when the latter is considered for all wave numbers k_x, k_y. Hence, the solution $\mathbf{W}$ to the Euler–Lagrange equations (19) now corresponds to a *saddle point*. We thus

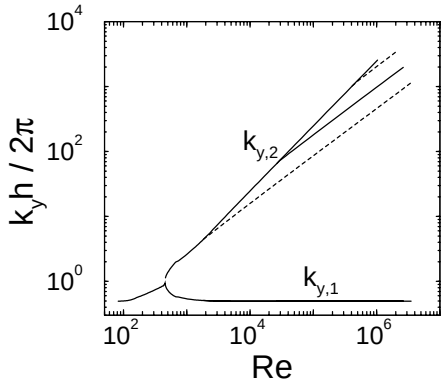

Fig. 4. Minimizing wave numbers k_y belonging to the optimal upper bound on the dissipation coefficient $c_\varepsilon(Re)$. The uppermost and the lowest solid line represent the wave numbers $k_{y,2}$ and $k_{y,1}$ furnished by the unmodified variational principle. The full line that bifurcates at $Re \approx 3 \times 10^4$ from the upper line is the wave number $k^*_{y,2}/(2\pi/h) \approx 0.040 \times Re^{0.73}$ resulting from the modified principle for $b = 10$ (fit to the data; the asymptotic exponent is 0.706(3)). The two adjacent dashed lines indicate the analogous results for $b = 5$ (upper dashed line) and $b = 20$ (lower dashed line). The data for $k^*_{y,1}$ with $b = 5$, 10, and 20 are almost equal to $k_{y,1}$. The wave numbers are plotted in multiples of $2\pi/h$.

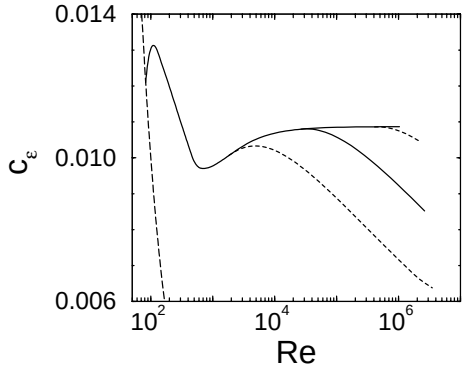

Fig. 5. Bound on $c_\varepsilon(Re)$ obtained from the original variational principle (upper full line) compared to the new bound resulting from the modified principle for $b = 10$ (lower full line; corresponding to the short-dashed line in Figure 1.) The two short-dashed lines indicate the analogous results for $b = 5$ and $b = 20$; the long-dashed line on the left is the lower bound (6). Note the linear ordinate. (The data for $b = 20$ seem to change their slope for $Re > 10^6$. Since this occurs only at the very limit of the regime where our numerical routines can work reliably, we consider this to be an artifact.).

rely on the assumption that every eigenvector furnished by a self-consistently computed ϕ, which belongs to an eigenvalue that has passed zero and has become negative, remains associated with unphysically large wave numbers, so that the solution to the Euler–Lagrange equations (19), although being a saddle-point with respect to the entire **V**-space, still corresponds to the minimum of its physically accessible subset. Therefore we use the solution to equation (19) precisely as we did in the previous procedure, and arrive at the same bounding graphs (28) also for the self-consistent profiles, so that the subsequent lower-envelope construction remains formally unchanged.

In Figure 4 we compare the minimizing wave numbers $k^*_{y,2}$ and $k^*_{y,1}$ that result from the numerical solution of the self-consistency problem to the minimizing wave numbers $k_{y,2}$, $k_{y,1}$ furnished by the unmodified variational principle, represented by the uppermost and lowest solid lines. The additional solid line bifurcating at $Re \approx 3 \times 10^4$ from the upper one indicates $k^*_{y,2}$ for $b = 10$. A fit to the power law

$$\frac{k^*_{y,2}}{2\pi/h} \sim C\, Re^{\gamma} \tag{39}$$

shows that these numerical data are well described by

$$C \approx 0.040 \quad \text{and} \quad \gamma \approx 0.73. \tag{40}$$

More careful data inspection reveals that these parameters do not describe the true asymptotic behavior of $k^*_{y,2}$; as argued in Appendix A, one expects an exponent $\gamma_\infty = 0.706(3)$ in the asymptotic regime. Nonetheless, we state the "local" values of C and γ here, valid for Reynolds numbers between roughly 10^5 and 10^7, since the asymptotics are reached only at unrealistically high Re (see also Appendix B for quite accurate, analogous results obtained for a simplified model). The two adjacent dashed lines mark $k^*_{y,2}$ for $b = 5$ and $b = 20$, respectively; they are described by the *same* exponent γ_∞ in the asymptotic regime. The data for $k_{y,1}$ and $k^*_{y,1}$ with $b = 5$, 10, and 20 are almost indistinguishable, so that they fall onto a single line.

Figure 5 shows, with linear ordinate, the corresponding upper bounds on the dissipation coefficient: The upper solid line represents the bound provided by the unmodified principle (which approaches the constant value (7) for large Re); the long-dashed line on the left is the lower bound (6) determined by the laminar flow. The additional solid line emerging at $Re \approx 3 \times 10^4$ indicates the improved bound obtained from the modified principle for $b = 10$; the displayed data are well fitted by

$$\overline{c_\varepsilon}(Re) \sim A\, Re^{-\alpha} \tag{41}$$

with

$$A \approx 0.027 \quad \text{and} \quad \alpha \approx 0.08. \tag{42}$$

Again, this is a *local* fit; the numerical data are consistent with the asymptotic value $\alpha_\infty = 0.18(1)$ (see Appendix A). The two short-dashed lines mark the bounds obtained for $b = 5$ and $b = 20$; they obey the same asymptotic power-law decrease. It should be noted that, as a consequence of the definitions (36, 37), the parameters A and α should be related to the parameters (40) by

$$A^{1/4}/C \sim b \quad \text{and} \quad \alpha = 3 - 4\gamma. \tag{43}$$

Both our local coefficients A and C and the local exponents α and γ obey these relations well, even though they do not describe the (in the mathematical sense) "true" asymptotics; the asymptotic exponents satisfy $\alpha_\infty = 3 - 4\gamma_\infty$, as required.

4 Discussion

One of the most interesting questions for judging the results produced by the variational principle is whether an optimal variational profile $\phi(\zeta)$ is somehow related to the time-averaged mean profile $\psi(\zeta)$ of the turbulent field $\mathbf{u}(\mathbf{x}, t)$. With increasing Reynolds number, the optimized profiles become flat in the interior (*i.e.*, the slope p parameterizing the optimized test profiles (33) approaches zero for $Re \to \infty$), and steep in the vicinity of the boundaries; for the case of the original variational principle we have shown previously that the variational parameter n becomes proportional to Re at high Reynolds numbers, whereas p vanishes proportional to Re^{-1} [17–19]. Mean-flow profiles tend to behave similarly, but on the first glance there seems to be no obvious reason why the two types of profiles should exhibit more than just a superficial resemblance. The only mathematical argument encountered so far which connects the optimal auxiliary field $\mathbf{U}$, and hence its profile ϕ, to a time average arises from the estimate (18): $\mathbf{U}$ should be chosen such that after inserting the turbulent deviations $\mathbf{v} = \mathbf{u} - \mathbf{U}$ into the integrand on the left hand side of (18) and averaging over time, one comes as close as possible to the expression obtained when replacing $\mathbf{v}$ by the minimizing stationary field $\mathbf{V} = \mathbf{W}\{\mathbf{U}\}$. Nonetheless, at least one more direct statement can be made. It rests on the observation that the true dissipation rate ε is related to the derivative $\psi'(0)$ of the (normalized) mean-flow profile at the boundary by means of the identity

$$c_\varepsilon(Re\,) = \frac{\psi'(0)}{Re}, \tag{44}$$

which follows directly from the Navier–Stokes equations by dotting with $\mathbf{u}$ and averaging over both the volume $\Omega = L_x L_y h$ and time. A similar expression connecting the upper bound $\overline{c_\varepsilon}(Re\,)$ and the derivative $\phi'(0)$ of the optimized variational profiles can be found at least in the regime of asymptotically high Re, if one recalls that there exists a systematic expansion of the bound in terms of the profile functional (27) and the rescaled Reynolds number (26) (stated as Eqs. (3.3, 3.4) in Ref. [19]). This expansion reduces to

$$\overline{c_\varepsilon}(Re\,) \sim \frac{27}{16}\,\frac{D\{\phi\}}{R} \tag{45}$$

and

$$R \sim \frac{3}{2}\,Re \tag{46}$$

for high Re; the symbol "$\sim$" indicates asymptotic equality. Hence, we have

$$\overline{c_\varepsilon}(Re\,) \sim \frac{9}{8}\,\frac{D\{\phi\}}{Re}, \tag{47}$$

where the argument of D is that profile which yields the optimal bound at Re. It should be noted that this expression holds *both* for the unmodified *and* the modified principle (although, of course, the optimal ϕ are different in these two cases), since the two principles differ only in the admitted profiles ϕ, but not in the way the bound is constructed after the admissibility has been ascertained. The relation between the profile functional $D\{\phi\}$ and the boundary slope $\phi'(0)$ depends on the specific test profiles used. Inserting our test profiles (33), the profile functional becomes

$$D\{\phi\} = \left[\frac{1}{2}\,\frac{n^2}{(2n-1)\,\delta} - 1\right](1-p)^2 \sim \frac{n}{4\,\delta}, \tag{48}$$

keeping in mind that p vanishes asymptotically, while n becomes large. On the other hand, one finds

$$\phi'(0) = p + \frac{n}{2\delta}\,(1-p) \sim \frac{n}{2\,\delta}, \tag{49}$$

implying

$$D\{\phi\} \sim \frac{1}{2}\,\phi'(0). \tag{50}$$

Thus, the relation (47) leads to the asymptotic analogue of equation (44),

$$\overline{c_\varepsilon}(Re\,) \sim \frac{9}{16}\,\frac{\phi'(0)}{Re}\,. \tag{51}$$

Since $c_\varepsilon(Re\,) \le \overline{c_\varepsilon}(Re\,)$, one now deduces the asymptotic inequality

$$\phi'(0) \ge \frac{16}{9}\,\psi'(0) \quad \text{for} \quad Re \to \infty, \tag{52}$$

stating that the derivative of the optimized variational profile at the boundary has to become strictly larger than that of the mean-flow profile. It appears remarkable, though, that the lowest possible factor $16/9 \approx 1.78$ by which $\phi'(0)$ has to exceed its mean-flow counterpart at high Re is merely a Re-independent number of the order of unity, so that the optimal profiles produced by the variational principle can actually share some properties of the physically realized mean profiles $\psi(\zeta)$.

Apart from its conceptual importance, the asymptotic relation (51) can also be exploited for checking the consistency of our numerical routines. Our data for $\phi'(0)$, as obtained from the modified variational principle with the cutoff parameter $b = 10$, are well described by the local fit

$$\phi'(0) \sim B\,Re^{\beta} \tag{53}$$

with

$$B \approx 0.047 \quad \text{and} \quad \beta \approx 0.92; \tag{54}$$

they are plotted, together with the corresponding data for $b = 5$ and $b = 20$ and those provided by the unmodified principle, in Figure 6. (The expected asymptotic value of the exponent is $\beta_\infty = 0.82(2)$). Whereas the previous relations (43) between the parameters C and γ characterizing the upper minimizing wave number $k^*_{y,2}$ and the parameters A and α describing the dissipation bound $\overline{c_\varepsilon}$ were

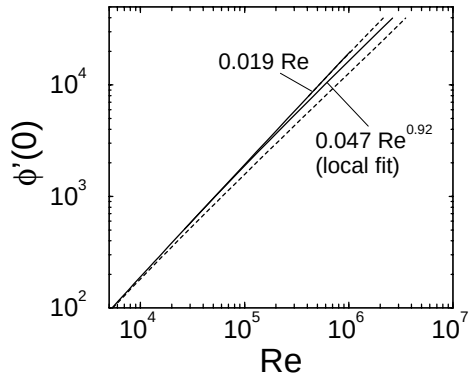

Fig. 6. Boundary slope $\phi'(0)$ of the optimized profiles pertaining to the unmodified variational principle (upper full line: $\phi'(0) \sim 0.019 \times Re$; the coefficient 0.019 is 16/9 times the value of the asymptotic bound (7)), and to the modified principle with $b = 10$ (lower full line; the data are fitted by $\phi'(0) \approx 0.047 \times Re^{0.92}$, while the asymptotic value of the exponent is 0.82(2)). The two dashed lines indicate the slopes obtained from the modified principle with $b = 5$ (upper dashed line) and $b = 20$ (lower dashed line).

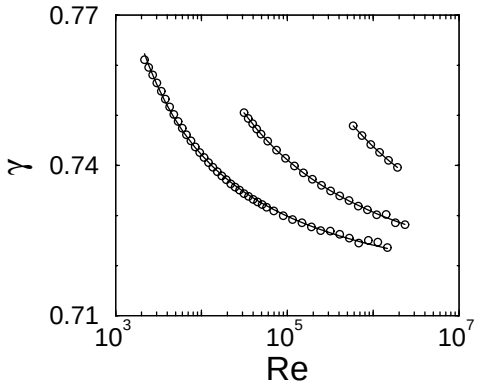

Fig. 7. Local exponents $\gamma(Re)$ obtained from the numerical raw data (circles) for $b = 5$, 10, and 20 (top to bottom). The solid lines indicate fits to the function (A.2). The coefficient a_0 is almost the same for each of the three data sets, thus giving the asymptotic exponent $\gamma_\infty = 0.706(3)$. Note that this value will be reached only at Reynolds numbers that are significantly higher than those accessible to our numerics.

merely a consequence of the definitions (36) and (37), the relations

$$A/B \sim 9/16 \quad \text{and} \quad \beta = 1 - \alpha \tag{55}$$

demanded by the asymptotic identity (51) constitute a more stringent test of our numerical results. Obviously, the local exponents $\alpha \approx 0.08$ and $\beta \approx 0.92 = 1 - 0.08$ obtained directly from fits to the respective raw data pass this test very well; even the ratio of the coefficients A and B does not fail.

The compliance of both the local exponents α, β, and γ and their asymptotic limits stated in Appendix A with the two relations $\alpha = 3 - 4\gamma$ and $\beta = 1 - \alpha$ indicates that these exponents have been determined correctly. Thus, the power-law decrease (41) of the bound on the dissipation coefficient, with its b-independent asymptotic exponent α, has to be taken seriously; this is what the self-consistently modified variational principle has to offer. It seems appropriate to re-emphasize that this bound still stands on somewhat shaky feet, since our argument is lacking mathematical rigor. Hence, some caution is still advised, and further work along the lines suggested in this work is clearly necessary. From the viewpoint of the physicist, the insight gained by giving up formal rigor is substantial. Already our local exponent $\alpha \approx 0.08$, valid around $Re \approx 10^6$, is more than twice as large as the exponent $\kappa \approx 0.035$ which, according to reference [9], could be implied by intermittent fluctuations; the asymptotic value $\alpha_\infty = 0.18(1)$ exceeds κ by a factor of more than five. This is no contradiction: That latter work is concerned with homogeneous isotropic *bulk* turbulence, whereas here we consider the *total* volume-averaged dissipation rate of *wall-bounded* shear flow; in fact, our crucial length scale $2\pi/k_{y,2}$, the consideration of which led to the lowering of the dissipation bound, is intimately linked to the extension of the variational profiles' boundary segments [19]. This is a serious indication that some signatures of shear-driven, wall-bounded turbulence might differ substantially from those implied by the theoretical ideal of homogeneous, isotropic turbulence.

This work was supported by the Deutsche Forschungsgemeinschaft *via* the Sonderforschungsbereich "Nichtlineare Dynamik", SFB 185.

Appendix A: Asymptotics of the dissipation bound

In order to extract the parameters A_∞ and α_∞ governing the asymptotic behavior of the bound $\overline{c_\varepsilon}(Re)$ from our numerical raw data $\{Re_j\,,\,\overline{c_\varepsilon}(Re_j)\}$ (where the index j labels successive data points), we first consider "local" exponents given by

$$-\alpha(Re_j) \equiv \frac{\ln \overline{c_\varepsilon}(Re_{j+1}) - \ln \overline{c_\varepsilon}(Re_j)}{\ln Re_{j+1} - \ln Re_j}\,; \tag{A.1}$$

local exponents $\beta(Re)$ and $\gamma(Re)$ describing the boundary slope $\phi'(0)$ and the upper minimizing wave number $k^*_{y,2}/(2\pi/h)$ are defined analogously. As shown in Figure 7 for the example of $\gamma(Re)$, even for the highest Reynolds numbers accessible to our numerics the exponents thus obtained have still not settled down to their asymptotic values. We therefore fit the local exponents to the function

$$f(Re) = a_0 + \frac{a_1}{a_2 + \ln Re}\,; \tag{A.2}$$

the quality of these fits is confirmed by the solid lines in Figure 7. It turns out that in all three cases — that is, when fitting $\overline{c_\varepsilon}$, $\phi'(0)$, or $k^*_{y,2}/(2\pi/h)$ — the respective parameter a_0 adopts almost the same value for $b = 5$, 10, and 20. In this way, we obtain reliable, b-independent

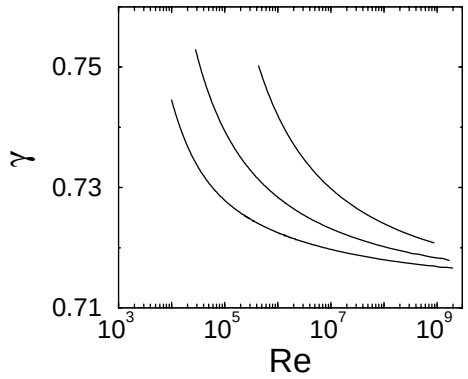

Fig. 8. Local exponents $\gamma(Re)$ for the two-dimensional model without spanwise degrees of freedom, for $b = 5$, 10, and 20 (top to bottom). Fits to the five-parameter-function (B.1) result in graphs that are indistinguishable from the numerical raw data displayed in the figure. The three fits consistently provide the value $a_0 = 0.709(1)$ for the asymptotic exponent γ_∞. This asymptotic value lies still significantly below the values reached at $Re = 10^9$.

estimates for the asymptotic exponents:

$$\alpha_\infty = 0.18 \pm 0.01, \tag{A.3}$$
$$\beta_\infty = 0.82 \pm 0.02, \tag{A.4}$$
$$\gamma_\infty = 0.706 \pm 0.003. \tag{A.5}$$

However, the physical significance of these numbers has to be questioned, since the asymptotics are reached rather slowly: According to our fit we expect, for instance, $\alpha(10^{10}) \approx 0.13$ and $\alpha(10^{20}) \approx 0.16$. Because of equations (43, 55), β and γ exhibit the same creeping convergency.

The asymptotic coefficients A_∞, B_∞, and C_∞ are then found in the same manner, *i.e.*, by introducing local coefficients $A(Re)$, $B(Re)$ and $C(Re)$, and employing the same fitting function (A.2). Of course, these coefficients do depend on the cutoff parameter b; we state the approximate asymptotic values for $b = 10$ here:

$$A_\infty \approx 0.34, \tag{A.6}$$
$$B_\infty \approx 0.61, \tag{A.7}$$
$$C_\infty \approx 0.063. \tag{A.8}$$

Obviously, the required relation $A_\infty^{1/4}/C_\infty \sim b$ is not obeyed too well. However, it must be borne in mind that to determine these coefficients constitutes a serious extrapolation; the asymptotic values A_∞ and B_∞ exceed the values of $A(10^6)$ and $B(10^6)$ by more than a factor of 10.

Appendix B: Asymptotic exponents for a 2-dimensional model

A useful model for exploring the variational principle for the upper bound on the dissipation rate in plane Couette flow is obtained if one omits the spanwise degrees of freedom, *i.e.*, if one artificially fixes the wave number k_y to zero. The properties of the resulting 2-dimensional model system are remarkably similar to those of the full problem [18,19]. In particular, its minimizing wave numbers k_x show the same bifurcation as the minimizing wave numbers k_y in the case of the unrestricted system. Since the restriction $k_y \equiv 0$ implies a drastic simplification of the mathematics, the model problem lends itself to both detailed asymptotic analysis [19] and numerical treatment at Reynolds numbers well above 10^7. In Figure 8 we display our results for this model's local exponents $\gamma(Re)$, defined as in Appendix A and computed with the same two-parameter test profiles as employed in reference [18]. Note that the numerical data span five decades of Reynolds numbers; the quality of the data is signaled by the smoothness of the curves. Fits to the five-parameter function

$$g(Re) = a_0 + \frac{a_1}{a_2 + \ln Re} + \frac{a_3}{(a_4 + \ln Re)^2} \tag{B.1}$$

result in graphs that are practically indistinguishable from the raw-data curves drawn in the figure; all three fits consistently yield the same value $a_0 = 0.709(1)$ for the asymptotic exponent γ_∞. Fitting the data for the model's self-consistent bound $\overline{c_\varepsilon}$ and the boundary slope $\phi'(0)$ to the same function (B.1), we obtain

$$\alpha_\infty = 0.164 \pm 0.002, \tag{B.2}$$
$$\beta_\infty = 0.836 \pm 0.004, \tag{B.3}$$
$$\gamma_\infty = 0.709 \pm 0.001. \tag{B.4}$$

These asymptotic exponents of the model are well compatible with the relations $\alpha = 3 - 4\gamma$ and $\beta = 1 - \alpha$, and even agree, within the error bars, with the exponents provided by the unrestricted system.

Clearly, more illustrative than the actual numerical values of the exponents is their creeping approach to the asymptotics: As seen in Figure 8, even at $Re = 10^9$ the local value of γ (with $b = 10$) is still about 0.718. The regime of Reynolds numbers ranging from $Re = 10^7$ to 10^9 is actually well described by $\gamma \approx 0.72$, giving a local exponent $\alpha \approx 0.12$ which is only about three quarters of its asymptotic value. This indicates once more that the mathematically proper asymptotics might not be reachable with physically accessible Reynolds numbers.

References

1. L.N. Howard, Annu. Rev. Fluid Mech. **4**, 473 (1972).
2. C.R. Doering, P. Constantin, Phys. Rev. E **49**, 4087 (1994).
3. K.R. Sreenivasan, Phys. Fluids **27**, 1048 (1984).
4. D.P. Lathrop, J. Fineberg, H.L. Swinney, Phys. Rev. Lett. **68**, 1515 (1992).
5. D.P. Lathrop, J. Fineberg, H.L. Swinney, Phys. Rev. A **46**, 6390 (1992).
6. B. Castaing, G. Gunaratne, F. Heslot, L. Kadanoff, A. Libchaber, S. Thomae, X.-Z. Wu, S. Zaleski, G. Zanetti,

J. Fluid Mech. **204**, 1 (1989).
7. X.-Z. Wu, A. Libchaber, Phys. Rev. A **43**, 2833 (1991).
8. D. Lohse, Phys. Rev. Lett. **73**, 3223 (1994).
9. S. Grossmann, Phys. Rev. E **51**, 6275 (1995).
10. E. Hopf, Math. Annalen **117**, 764 (1941).
11. F.H. Busse, J. Fluid Mech. **41**, 219 (1970).
12. F.H. Busse, Adv. Appl. Mech. **18**, 77 (1978).
13. P. Constantin, C.R. Doering, Phys. Rev. E **51**, 3192 (1995).
14. C.R. Doering, P. Constantin, Phys. Rev. E **53**, 5957 (1996).
15. R. Nicodemus, S. Grossmann, M. Holthaus, Physica D **101**, 178 (1997).
16. R. Nicodemus, S. Grossmann, M. Holthaus, Phys. Rev. Lett. **79**, 4170 (1997).
17. R. Nicodemus, S. Grossmann, M. Holthaus, Phys. Rev. E **56**, 6774 (1997).
18. R. Nicodemus, S. Grossmann, M. Holthaus, J. Fluid Mech. **363**, 281 (1998).
19. R. Nicodemus, S. Grossmann, M. Holthaus, J. Fluid Mech. **363**, 301 (1998).
20. R.R. Kerswell, Physica D **100**, 355 (1997).
21. H. Reichardt, *Gesetzmäßigkeiten der geradlinigen turbulenten Couetteströmung.* Mitteilungen aus dem Max–Planck–Institut für Strömungsforschung, Göttingen, **22** (1959).
22. D.D. Joseph, *Stability of Fluid Motions I & II* (Springer-Verlag, Berlin, 1976).
23. P.G. Drazin, W.H. Reid, *Hydrodynamic Stability* (Cambridge University Press, Cambridge, 1981).
24. B. Straughan, *The Energy Method, Stability, and Nonlinear Convection* (Springer-Verlag, New York, 1992).
25. L. Boberg, U. Brosa, Z. Naturforsch. **43a**, 697 (1988).
26. T. Gebhardt, S. Grossmann, Phys. Rev. E **50**, 3705 (1994).
27. L.N. Trefethen, A.E. Trefethen, S.C. Reddy, T.A. Driscoll, Science **261**, 578 (1993).
28. J.M. Hamilton, J. Kim, F. Waleffe, J. Fluid Mech. **287**, 317 (1995).
29. S. Grossmann, *The Onset of Shear Flow Turbulence* (Preprint, Philipps-Universität Marburg, 1999); Rev. Mod. Phys. (submitted).
30. H. Effinger, S. Grossmann, Z. Phys. B **66**, 289 (1987).